To be published in Conference Proceedings of
ICANS-X, Los Alamos, NM, 3-7 Oct. 1988

BNL-42079

BNL/NPB-88-111

Pulsed–Neutron Production at the Brookhaven 200–MeV Linac*

T.E. Ward, J. Alessi,† J. Brennan,† P. Grand, R. Lankshear,
P. Montemurro,† C.L. Snead, Jr. and N. Tsoupas

BNL--42079

DE89 005664

Department of Nuclear Energy

Brookhaven National Laboratory, Upton, New York 11973

ABSTRACT

The new 750–kV RFQ preinjector and double chopper system capable of selecting single nanosecond micropulses with repetition rates of 0.1–20 MHz has been installed at the Brookhaven 200–MeV proton linac. The micropulse intensity is approximately 1×10^9 p/μpulse. Neutron time–of–flight path lengths of 30–100 meter at 0°, 12°, 30°, 45°, 90° and 135° are available as well as a zero degree beam swinger capable of an angular range of 0–25°. Pulsed neutron beams of monoenergetic ($p^7Li \rightarrow n^7Be$) and spallation ($p^{238}U \rightarrow nx$) sources will be discussed in the present paper as well as detailing the chopped–beam capabilities.

Introduction

The replacement of one of the Cockcroft–Walton preinjectors[1–3] with a new high–current 750–keV radiofrequency quadrupole (RFQ) will improve substantially the H^- capabilities of the Brookhaven 200–MeV Linac.[1–3] In conjunction with the new RFQ a double chopper capable of single–micropulse selection (pulse width <1 ns) with periods ranging from 100 ns to greater than 10 μs will be installed. The new double–chopper RFQ system is detailed in the present paper as well as the neutron–time–of–flight (NTOF) capabilities that exist at the 200–MeV Linac complex. Future improvements and upgrades that will also be described include a 0–30° beam swinger on the zero–degree line and intense pulsed monoenergetic and spallation neutron sources for use in nuclear physics and radiation–effects studies.

The Double–Chopper RFQ System

The RFQ Linac input is from a 35–keV H^- magnetron ion source modified to produce an axially symmetric beam matched to the RFQ. The RFQ parameters are summarized in Table 1. Operational tests have routinely produced outputs of 50 mA from the RFQ, whereas the design current limit is rated at ~100 mA. The RFQ emittance at 50 mA was optimized for transport to the 200–MeV Linac.

Figure 1 shows an illustration of the double–chopper RFQ system. A fast beam chopper (Chop I) located between the ion source and the RFQ can variably bunch structure the beam with frequencies of 2.5 MHz or less. The first chopper is a slow–wave electrostatic deflection device that rejects the beam at a small aperture located before the RFQ. The second chopper (Chop II) is located after the RFQ and is phase locked to the RFQ. Chop II is a fixed–frequency sine–wave chopper that selects single microbunches (440 ps width) of the 200–MHz RFQ Linac. The duty

*Work performed under the auspices of the U.S. Department of Energy under Contract No. DE-AC-02-76CH00016.

†AGS Department.

factor of the double chopper is adjustable from one bunch every 100 ns to one bunch per 450 μs macropulse. The macropulse frequency is 5 Hz. The standard 200–MHz micropulse intensity with 50 mA averaged current is 1.2×10^9 protons/μpulse. The dc–averaged beam current with 10–μs repetition rate and 5–Hz macrostructure is 50 nA, a value comparable with a 10–μsec 200–MeV pulsed beam from a cyclotron such as the Indiana University Cyclotron.

Table 1
RFQ Parameters:

Ion	H^+H^-
Input Energy	35 keV
Output Energy	753 keV
Current Limit	~100 mA
Operating Frequency	201.25 MHz
Peak Cavity Power	100 kW
Stored Energy	0.5 Joules
Duty Factor	0.007
Structure	4–vane, ringed
Vane Length	1.62 m

Figure 1. Double–Chopper RFQ Showing Single–Micropulse Selection

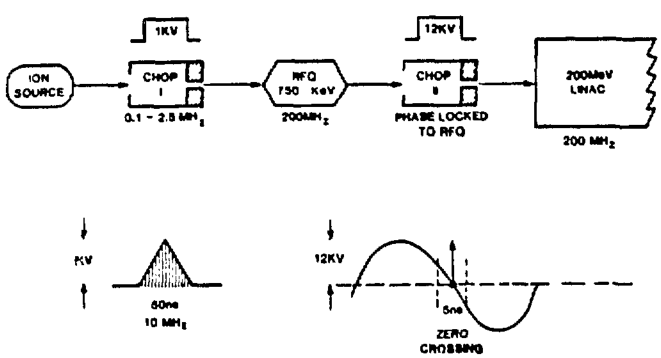

200–MeV Linac Performance

The Linac can accelerate H^+ or H^- beams of 92.6, 116.5, 139.0, 160.5, 181.0 and 200.3 MeV with an energy spread of about 140 keV at 200 MeV.[3] The standard operating beam at 200 MeV is a 30–mA peak current and 450–μs–wide macropulse. The repetition rate is currently 5 pps but can be increased to 7–8 pps. The microstructure is 200 MHz or 1 μpulse every 5 ns with a μpulse width <1 ns. The typical beam spot is 1.5 cm FWHM Gaussian in both vertical and horizontal dimensions yielding a flux of approximately 9×10^{12} p/sec·cm^2.[2] The maximum total beam current per macropulse is about 10 μA dc averaged.

The adjustable parameters are the macropulse (5 μs–500 μs), the peak current (1 mA–30 mA), the transported beam (1 nA–10 μA) and beam size (3 cm^2–7850 cm^2) delivered to the target areas of the Radiation Effects Facility (REF) and Neutral Beam Test Facility (NBTF).

<u>NTOF Facilities and Performance</u>

The 200–MeV Linac complex consists of NTOF facilities at the Radiation Effects Facility (REF) and Neutral Beam Test Facility (NBTF) as shown in Fig. 2. The REF has 30–100–m flight paths at 12, 30, 45, 90, and 135° with approximately 30 m of earth shielding (12" tubes through shielding). The zero–degree line located at the NBTF consists of a 3-m diameter underground tunnel with a present length of 100 m, a zero–degree sweep and dump magnet, and a collimation wall (3 m thick).

Figure 2. BNL 200–MeV Linac Complex.

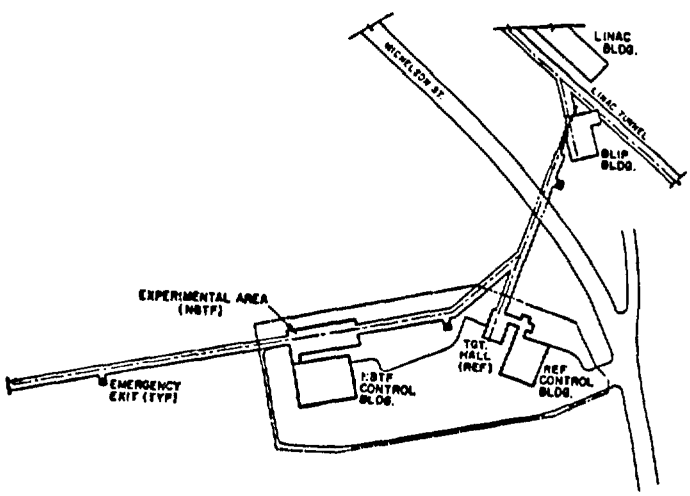

The momentum spread in the beam ($\Delta p/p = 7 \times 10^{-4}$), coupled with the 125–m beam transport into the REF and NBTF, increases the width of the micropulse to about 1 ns from the intrinisic width of 440 ps which results from the Linac acceleration. The overall NTOF energy resolution (ΔE_n) that results from a combination of the micropulse width (~1 ns), detector timing resolution (0.8 ns), and the detector width (see Ref. 4 for details) is shown in Fig. 3 for various flight paths and neutron energies. The detector width contributes 58–82% to the uncertainty in the 200–10–MeV neutron energy range, respectively.[4–6] The overall resolution is somewhat less than that of other intermediate–energy (p, n) facilities but uniquely provides high dc–averaged beam currents with repetition rates of 100 ns–10 μs or greater. These low–frequency micropulse modes, with 100-kHz rates and 100–m path lengths, allow the NTOF spectral range of E_n = 1–200 MeV to be acquired without troublesome wraparound backgrounds.

Figure 3. NTOF Energy Resolution as a Function of Neutron Energy and Flight Path

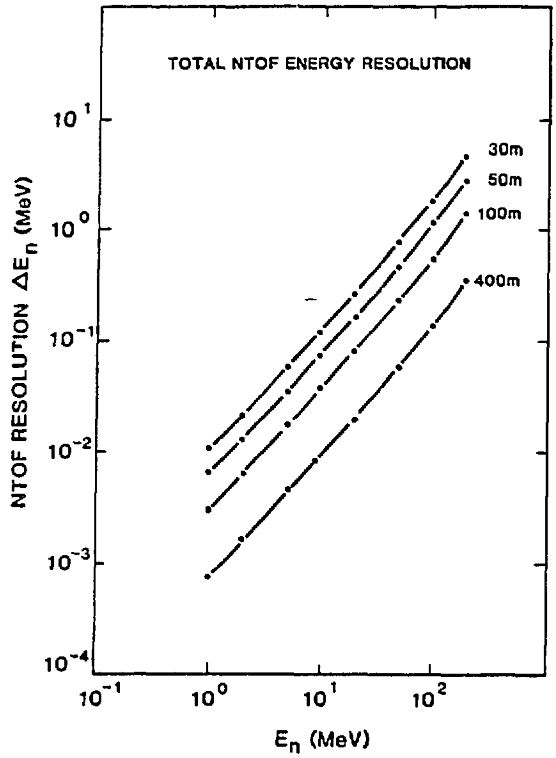

The zero-degree NTOF sweep magnet in the NBTF line is a large-aperture (31.5-cm gap) high-field magnet (1.9 T) that allows target insertion along the beam trajectory permitting the forward neutron angles of 0–25° to be selected. The protons after interacting with the target are transported to a proton Faraday cup shielded in the target hall. The forward-directed neutrons emerge through a collimation wall (3-m width) for transport in vacuum through the 100-m TOF tunnel.

Monoenergetic and Spallation Pulsed Neutron Beams

The facility can produce intense pulsed monoenergetic netron beams of 93–200 MeV. The nearly monoenergetic neutrons are produced in the $^7Li(p, n)^7Be$ (0.0 and 0.43 MeV) charge-exchange reaction. Lithium produces copious quantities of neutrons, has only one excited state, and little continuum neutron production. The differential cross section for $E_p = 120$ MeV is shown in Fig. 4 (ref. 7). The reaction is strongly forward peaked, has a total reaction cross section dependence on the proton energy of $E^{-1.13}$ in the E_p = 60–800-MeV range,[8] and a zero-degree cross section of $d\sigma/d\Omega = 35 \pm 1$ mb/sr. The maximum neutron yield from a 210 mg/cm^2 ^7Li metal target would be 1.5×10^6 n/sr per micropulse or about 7.5×10^{10} n/sr s.

Figure 4. Angular distribution for the $^7Li(p, n)^7Be$ (g.s. + 0.43 MeV) reaction obtained at $E_p = 120$ MeV. (Ref. 7.)

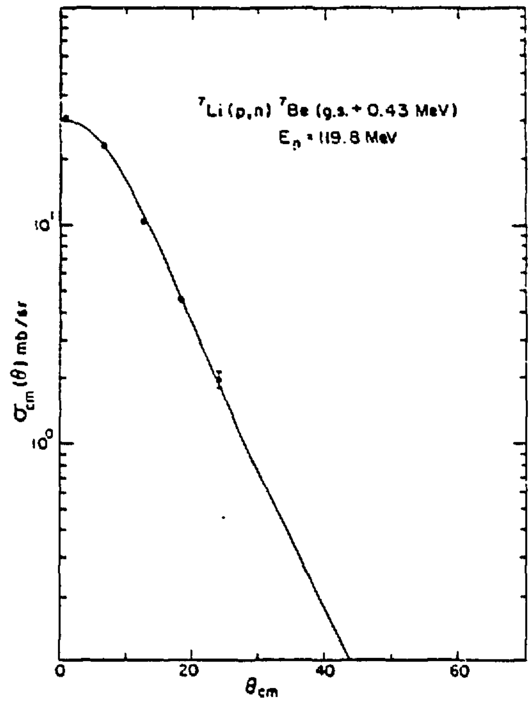

The 200-MeV proton beam at the BNL Radiation Effects Facility (REF) can also produce an intense fission–spallation spectrum of neutrons. This is accomplished by using a depleted uranium (U–238) target to stop the beam. The spectral comparison[9] with a pure thermal fission spectrum are shown in Fig. 5 where the main difference between an actual thermal fission spectrum are the high–energy spallation (p, n) direct components. The direct components yields are typically (5–10%) of the total neutron yield. The spallation target consists of a 15 cm × 15 cm × 4 cm slab of depleted ^{238}U that has an area density of 74 g/cm^2 which is greater than 110% the range of a 200–MeV proton. The ^{238}U (p, fission) cross section is essentially constant at energies greater them $E_p = 20$ MeV and is given as 1.44 ± 0.10 b.[10] The total inelastic (fission and spallation) cross section is 1.91 b.[11] The total neutron yield is approximately 6.4 × 10^{10} n/sr per micropulse or 3 × 10^{15} n/sr s for full beam intensity.

Figure 5. Comparison of ^{235}U thermal fission neutron spectrum and 200 MeV p + ^{238}U spallation neutron spectrum.

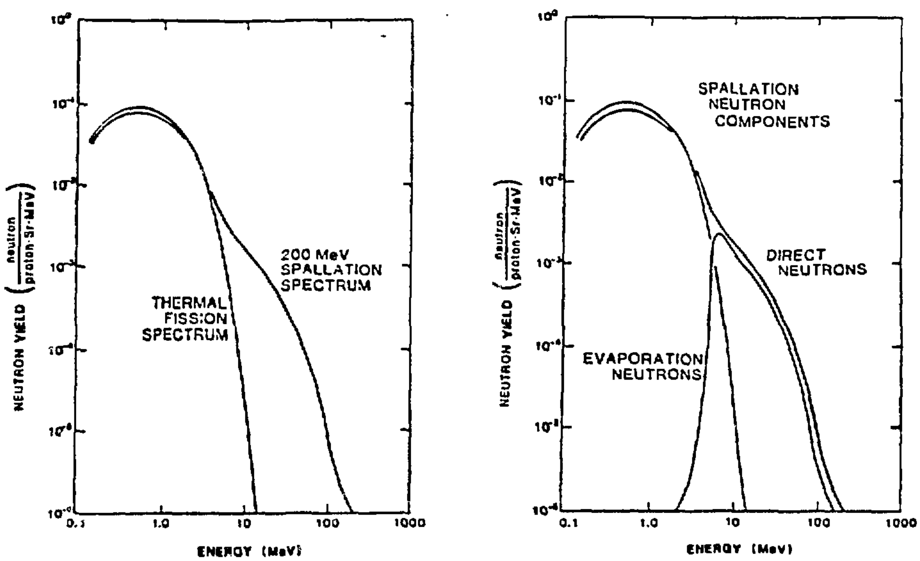

Pulsed monoenergetic or spallation (fission) source neutron beams are of considerable current interest in intermediate–energy (n, p) nuclear physics research, for use in radiation–effects studies of electronics or other material flown in space, or research on materials used in fusion or fission reactors. The BNL radiation–effects facilities (REF and NBTF) can provide for a wide range of experimental conditions, the advantages of the user facility being:

1. Controlled Radiation Environment. Beam size and intensity can vary to meet wide range experimenters needs.

2. Reproducibility. Experiments can be readily repeated to assure reproducible results.

3. Flexible User Experimental Schedule. Beam available on demand with reasonably short lead times.

In summary, the REF/NBTF complex can uniquely provide high–intensity pulsed (<1 ns) and macropulse (500 μs) proton beams of 93–200 MeV. Furthermore, the use of appropriate targets of ^{7}Li or ^{238}U can produce monoenergetic and spallation neutron beams, respectively, that can likewise be pulsed or macropulsed. These beams can be expanded from 2 cm to 1 m in diameter in radiation–effects studies of systems, subsystem, or components.

References

1. Design of an RFQ for BNL/FNAL, R. Gough et al., 1986 Linac Conference, Abstract #WE 3–8, to be published.

2. J.G. Alessi, et al., Proc. IEEE Part. Accel. Conference **1**, 276 (1987), and **1**, 304 (1987).

3. G.W. Wheeler, K. Batchelor, R. Chasman, P. Grand, and J. Sheehan, PLACBD **9**, 1 (1979).

4. T.N. Taddeucci, *Proc. AIP Conf #124*, pg. 394 (1985), J. Rapaport, R.W. Finlay, S. Grimes, and F. Deitrich, editors (AIP, New York 1985).

5. C.D. Goodman, J. Rapaport, D. Bainum, M. Greenfield, and C. Goulding, IEEE **NS–25**, 577 (1978).

6. C.D. Goodman, J. Rapaport, D. Bainum, and C. Brient, NIM **151**, 125 (1978).

7. C.A. Goulding, M.B. Greenfield, C.C. Foster, T.E. Ward, J. Rapaport, D.E. Bainum, and C.D. Goodman, Nucl. Phys. **A331**, 29 (1979).

8. J. D'Auria, M. Dombsky, L. Moritz, T. Ruth, G. Sheffer, T.E. Ward, C.C. Foster, J. Watson, B. Anderson, and J. Rapaport, Phys. Rev. **C30**, 1999 (1984).

9. "Monte Carlo High Energy Nucleon–Meson Transport Code System," HETC, ORNL–CCC–178, 1977.

10. *The Nuclear Properties of the Theory Elements*, Vol. III, Fission Phenomena, Prentice Hall, E.K. Hyde, Editor, Chapter 7, Section 4, 1964. *Ibid*, Chapter 9, *Ibid*, Chapter 11, Section 6.

11. P.J. Karol, Phys. Rev. **C11**, 1203 (1975).